Isr. J. Earth Sci.; 53: 187–197

Mapping saline groundwater beneath the Sea of Galilee and its vicinity using time domain electromagnetic (TDEM) geophysical technique

Mark Goldman,[a] Haim Gvirtzman,[b] and Shaul Hurwitz[c]
[a]Geophysical Institute of Israel, P.O. Box 182, Lod 71100, Israel
[b]Institute of Earth Sciences, The Hebrew University of Jerusalem, Jerusalem 95501, Israel
[c]USGS, Menlo Park, California 94025, USA

(Received 27 February 2003; accepted in revised form 22 February 2004)

ABSTRACT

Goldman, M., Gvirtzman, H., and Hurwitz, S. 2004. Mapping saline groundwater beneath the Sea of Galilee and its vicinity using time domain electromagnetic (TDEM) geophysical technique. Isr. J. Earth Sci. 53: 187–197.

An extensive time domain electromagnetic (TDEM) survey covering the Sea of Galilee with a dense grid of points has been recently carried out. A total of 269 offshore and 33 supplementary onshore TDEM soundings were performed along six N–S and ten W–E profiles and at selected points both offshore and onshore along the whole coastal line. The interpreted resistivities were calibrated with the direct salinity measurements in the Haon-2 borehole and relatively deep (5 m) cores taken from the lake bottom. It was found that resistivities below 1 ohm-m are solely indicative of groundwater salinity exceeding 10,000 mg Cl/l. Such low resistivities (high salinities) were detected at depths greater than 15 m below almost the entire bottom of the lake. At some parts of the lake, particularly in the south, the saline water was detected at shallower depths, sometimes at a few meters below the bottom.

Relatively high resistivity (fresh groundwater) was found along the margins of the lake down to roughly 100 m, the maximum exploration depth of the system. The detected sharp lateral contrasts at the lake margin between high and low resistivities coincide with the faults separating the carbonate and clastic units, respectively.

The geometry of the fresh/saline groundwater interface below the central part of the lake is very similar to the shape of the lake bottom, probably due to the diffusive salt transport from the bottom sediments to the lake water.

The above geophysical observations suggest different salt transport mechanisms from the sediments to the central part of the lake (diffusion) and from regional aquifers to the margins of the lake (advection).

INTRODUCTION

The Sea of Galilee is a fresh-water lake located within the Dead Sea Rift Valley. The lake supplies 500 million cubic meters of water per year, which is about 25% of Israel's annual consumption. The average salinity of the lake, expressed in chloride concentration, is approximately 230 mg Cl/l, an order of magnitude higher than the concentration in the Jordan River and other streams entering the lake. This order of magni-

E-mail: mark@gii.co.il

 0021-2164/04 $4.00

tude difference is a result of saline water sources entering the lake. The sources include onshore and offshore springs with chloride concentrations in the range of 300–18,000 mg/l (Gvirtzman et al., 1997; Rimmer et al., 1999), as well as areal seepage from sediments beneath the lake (Stiller, 1994).

The objective of this study was to delineate the saline groundwater beneath the lake using the surface marine modification of the time domain electromagnetic (TDEM) method. The method was used to map the spatial distribution of brines in the sediments below the lake. In order to achieve the objective, a dense grid of measurements including a total of 269 offshore and 33 supplementary onshore TDEM soundings were performed along six N–S and ten W–E profiles and at selected points both offshore and onshore along the whole coastal line (Fig. 1).

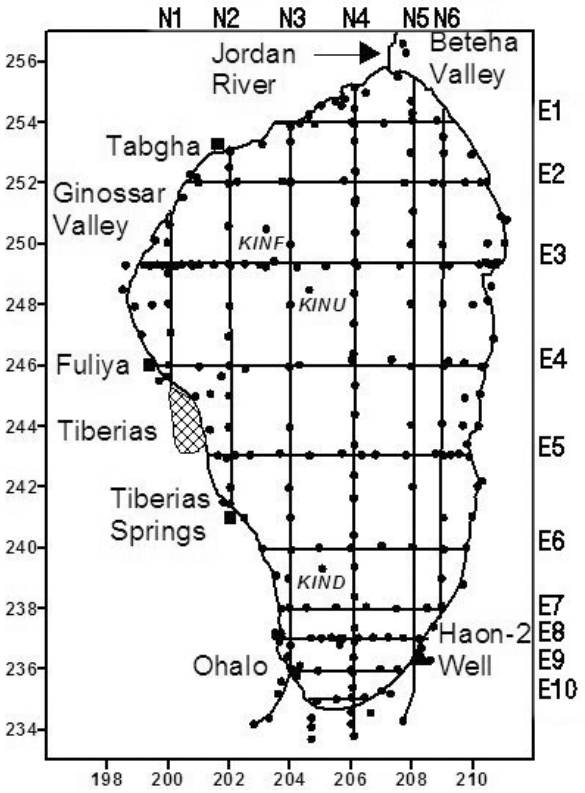

Fig. 1. Location map of the TDEM survey. Points designate locations of the TDEM soundings, which are grouped along N–S and W–E profiles. Labels on top and right side of the map are profile names. Locations of long cores (Stiller, 1994) and the appropriate correlation TDEM measurements are designated as KINF, KINU, and KIND.

HYDROGEOLOGICAL BACKGROUND

The Dead Sea Rift is a left-lateral strike-slip transform, separating the Sinai-Levant sub-plate from the Arabian plate (Garfunkel, 1981). The rift includes several en echelon rhomb-shaped grabens, one of which contains the Sea of Galilee, which is the lowest freshwater lake on Earth (210 m below msl).

Mesozoic to Tertiary sediments and Neogene to Quaternary basalt crop out in the highlands on both sides of the rift valley and constitute the recharge area of the regional aquifers. Most of the groundwater is drained to the rift valley through the limestone and dolomite aquifers of the upper Cretaceous to Eocene, which are separated from each other by aquitards of predominantly chalk and marl (Gvirtzman et al., 1997). Although faulted, these aquifers are laterally continuous (Fig. 2). The salinity in deep aquifers increases from less than 100 mg Cl/l in the highlands to more than 10,000 mg Cl/l in the downfaulted blocks (Mazor and Mero, 1969).

The subsiding basin in which the Sea of Galilee is seated (Fig. 2) is capped by a Miocene–Holocene sequence thicker than 6 km in the deepest part (Ben-Avraham et al., 1996), consisting of alluvial and lacustrine deposits, evaporites, and intrusive and extrusive igneous rocks (Marcus and Slager, 1985). These rocks are mainly aquitards, which obstruct flow through the regional aquifers (Fig. 2), forming two independent systems on the eastern and western sides of the basin (Arad and Bein, 1986). On the western margin, some faulted blocks expose the upper Cretaceous aquifer at three locations: Tabgha, Fuliya, and Tiberias Springs (Fig. 1). A few saline springs are located adjacent to these exposures. These springs discharge water with salinities ranging from a few hundred to about 20,000 mg Cl/l, and are a mixture of fresh and saline groundwater (Mazor and Mero, 1969; Issar, 1983). The fresh component drains latterly from the regional shallow aquifers, and the saline component from deeper aquifers (Fig. 2). On the other hand, on the eastern margin, low permeability sediments block discharge from the regional aquifers to outlets near the lake shore. A few boreholes (<200 m) along the eastern shore have revealed that water salinity ranges from a few hundred mg Cl/l to about 15,000 mg Cl/l (Shaharabani et al., 1980).

The average amount of Cl entering the lake under natural conditions is 150,000 tons per year (Simon and

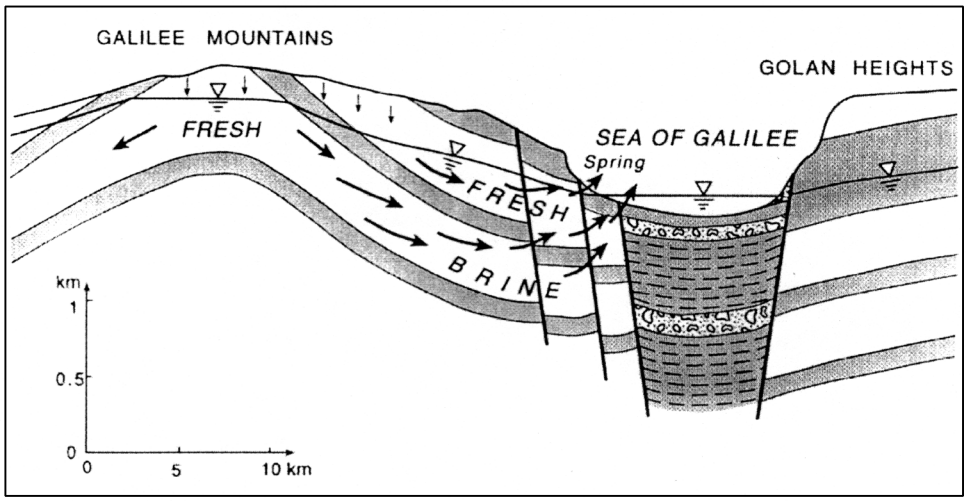

Fig. 2. Schematic hydrogeological cross section showing the groundwater sources of the saline springs at the western shore of the Sea of Galilee. The basin fill is an aquitard.

Mero, 1992). During the last few decades, about 56,000 tons (that emerge from some onshore springs) are diverted through an aqueduct before entering the lake (Assuline et al., 1994). Chloride contribution from surface streams is about 13,000 tons per year and therefore undiverted onshore and offshore springs and diffusion from the lake sediments contribute about 80,000 tons of Cl annually into the lake. The discharge location of the majority of these salts is unknown, as only a few offshore springs have been found.

Nineteen short cores (50 cm) and three long cores (500 cm) were dredged at various locations on the lake floor in order to examine their chloride content (Stiller, 1994). The water in all cores showed a roughly linear increase in chloride concentration from about 220 mg/l at the top of the core (water–sediment interface) to 350–600 mg/l at 50 cm, and 2000–3500 mg/l at 500 cm in the long cores (Fig. 3). A rough estimate based on the observed gradients in the cores has revealed a diffusion rate of 5.3 mg Cl cm^{-2} yr^{-1} from the lake bottom, resulting in an annual contribution of 9,000 tons of Cl from the base sediments of the lake by diffusion (Stiller, 1994). These results clearly indicate that saline units are located at shallow sub-bottom depths over large parts of the lake. However, their spatial distribution and actual sub-bottom depth are unknown.

From a practical point of view, the salinity of the lake water is too high for irrigation. Moreover, when lake water is pumped and recharged into the Coastal Plain aquifer for seasonal storage, it further increases the aquifer salinity (whose salinity ranges between 100–200 mg Cl/l). Therefore, great efforts have been and are presently devoted to decreasing the lake salinity. In order to further reduce the lake salinity, it is vitally important to evaluate quantitatively the spatial distribution of salt concentrations in the sediments beneath the lake floor as well as salt fluxes. This objective is fulfilled, at least in part, by using the proposed surface marine modification of the standard onshore time domain electromagnetic (TDEM) method.

MARINE TDEM SYSTEM

The conventional onshore TDEM system is well known and widely elucidated in the geophysical literature (e.g., Fitterman and Stewart, 1986; Goldman et al., 1991). The system consists of a transmitter and receiver. The transmitter is usually represented by a square loop of insulated wire laid on the surface. A multi-turn air coil (about 1 m in diameter) is placed either inside or outside the loop and serves as the receiver antenna. The array, in which the receiver coil is located in the center (central loop array), provides the most accurate data and best lateral resolution and

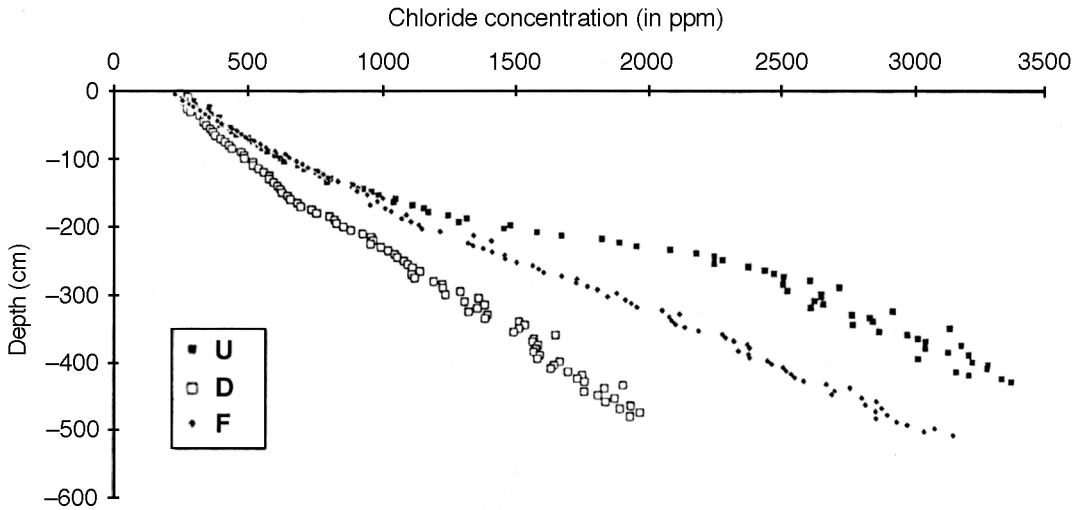

Fig. 3. Chloride concentration in the pore water of the 5-m-long cores versus depth (after Stiller, 1994). U, D, and F correspond to the locations designated in Fig. 1 as KINU, KIND, and KINF, respectively.

is, therefore, the most widely used configuration in TDEM soundings. The size of the transmitter loop usually varies between 50 × 50 meters for exploration depths of up to approximately 100 meters, and 500 × 500 meters for exploration depths of up to about 1000 m. It should be noted that the specified figures are very approximate and strongly depend on the geoelectric parameters and the noise level in the area.

The current waveform driven through the transmitter loop consists of equal periods of time-on and time-off. The emf is measured by a receiver coil during the transmitter "time-off" period only, thus providing the measurements of a purely secondary response, this being caused by the currents induced in the ground. As a result, the transmitter/receiver (T/R) separation in the TDEM method does not play as crucial a role as it does in all other controlled source geoelectric and geoelectromagnetic methods, in which the primary field, caused by the current in the transmitter antenna, must be removed or significantly reduced by increasing the T/R separation. In the TDEM method, the distance between transmitter and receiver can be less than half of the required exploration depth, and this unique feature of the method leads to significant improvement in lateral resolution and accuracy of measurements as compared to all other geoelectric and geoelectromagnetic techniques presently available.

In order to perform offshore TDEM measurements in the Sea of Galilee, a novel marine TDEM system has been developed (Goldman et al., 1996). The system consists of a 25-m-diameter circular transmitter loop, which floats on the water surface and is towed by a motorboat. Since the transmitter loop size was smaller than the minimum one (40 × 40 m) recommended by the equipment manufacturer (Geonics Ltd, Canada), several test measurements were carried out onshore using different sizes of the transmitter loop. It was shown that, due to the high conductivity of the subsurface material, the minimum transmitter loop size in the surveyed area can be much smaller than that recommended by Geonics (Goldman et al., 1996). The loop is constructed from a hermetically sealed PVC pipe, to which the transmitter current cable is tied using standard plastic clips. A 1-m-diameter receiver coil is rigidly connected to the center of the transmitter loop and to another rubber non-motorized boat, which is carrying an operator and a receiver console. Beside the coil and receiver console, there are no other metallic objects inside the transmitter loop. The navigation of the system is carried out by a differential GPS instrument. The latter, as well as the motor generator and the transmitter console, are located on the towboat outside the loop (Fig. 4).

Since the measurements with the suggested marine TDEM do not require assembling and disassembling of the system at each measuring point, the productivity of the survey is much greater than that of the conventional onshore TDEM (compare 30 to 40 offshore soundings per day with 6 to 8 onshore soundings per day). This, in turn, makes it possible to obtain more

detailed information and to increase the reliability of the interpretation, by carrying out the marine measurements along profiles rather than at isolated points as is typical of conventional surveys (though each offshore sounding is also being carried out in a stationary mode of operation). It should be noted that the first feasibility study measurements, using a relatively slow (10 to 15 soundings per day) marine TDEM system, were carried out along short selected profiles in 1994 (Goldman et al., 1996).

TDEM INTERPRETATION

The TDEM data collected at both onshore and offshore locations were processed and interpreted using two different 1-D inversion algorithms (Interpex Ltd., 1996). The first algorithm allows gradual resistivity change with increasing depth (smooth or Occam inversion; Constable et al., 1987). The second algorithm is for a layered earth model, in which sharp resistivity boundaries separate adjacent geoelectric layers.

Hydrogeologically, the former model is substantiated by the direct salinity measurements of Stiller (1994), showing a continuous increase of salinity with depth (Fig. 3). On the other hand, experience shows that smooth inversions are normally more ambiguous than layered ones and, in some cases, may even produce unrealistic geoelectric models.

In order to evaluate the benefits and shortcomings of each inversion algorithm, a comparative analysis of the smooth and layered interpreted models has been carried out at several locations. A typical example of such a comparison is shown in Figs. 5 and 6 for TDEM measurements KINF and KIND, respectively (the locations of the appropriate long cores are shown in Fig. 1). The most remarkable feature of both inversion schemes is the fact that the parameters of the geoelectric basement (very conductive lowermost half space) are detected almost uniquely irrespective to the distribution of the resistivities above the basement. It will be shown below that, from a hydrological viewpoint, the geoelectric basement is uniquely identified with the brine-saturated sediments beneath the lake bottom. Therefore, one might expect that the spatial distribution of brines will be accurately delineated by the TDEM measurements alone. The distribution of

Fig. 4. Marine TDEM system at the Sea of Galilee. The system consists of a 25-m transmitter loop and a small receiver coil located at the center. The coil is connected to the receiver console located in the rubber boat inside the loop. The current generator and the transmitter console are located in the towing motorboat.

resistivities above the basement and, particularly, their hydrogeological interpretation are somewhat more complicated issues.

The layered interpretation leads to a simple geoelectric model, which in most cases consists of three layers: an upper layer having a resistivity of about 10 ohm-m and a thickness slightly exceeding the bathymetry of the lake, a more conductive intermediate layer having a resistivity of 3 to 5 ohm-m and a thickness varying from several meters to a few tens of meters, and, finally, an extremely conductive geoelectric basement having a resistivity below (sometimes significantly) 1 ohm-m (Figs. 5 and 6).

It should be noted that similar models were obtained by means of layered interpretation in the overwhelming majority of the off-shore TDEM stations.

The smooth interpretation, however, shows both layering and gradual distribution of resistivity with depth, which fits fairly well the hydrological observations in some cases and could be obvious artifacts in the other cases. Indeed, comparison of Figs. 3, 5, and 6 suggests that smooth models may describe the salinity distribution below the lake bottom somewhat better than layered models (the salinity gradient in core F is similar to the resistivity gradient in KINF). At the same time, the significant resistivity contrasts, which occur within the water layer of the lake at locations KINF (just below the surface of the lake) and KIND (at a depth of approximately 15.5 m), are obvious artifacts of the smooth inversion (Figs. 5 and 6). Another artifact, although not so obvious, could be the distribution of smooth resistivities below the lake bottom at KIND (compare with the salinity gradient in core D) and the resistivity variations within the electric basement at both locations (Figs. 3, 5, and 6). The reasonable compromise would be thus to use smooth models for the hydrogeological interpretation, but to ignore those features that are not confirmed by the layered inversion.

It is important to emphasize that both interpretation methods are completely independent. Therefore the reliability of hydrogeological interpretation based on the use of only the common features of both models is greatly increased, although some features ignored by the layered

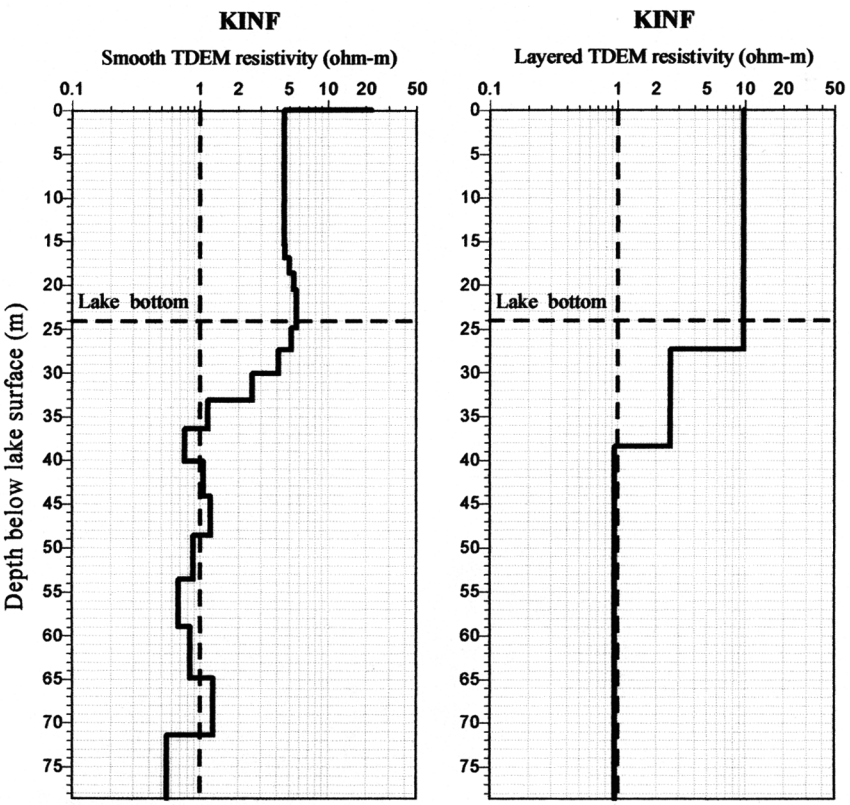

Fig. 5. Layered and smooth models interpreted at station KINF. Vertical dashed line represents threshold resistivity value for brine-saturated sediments. Horizontal dashed line shows the location of the lake bottom.

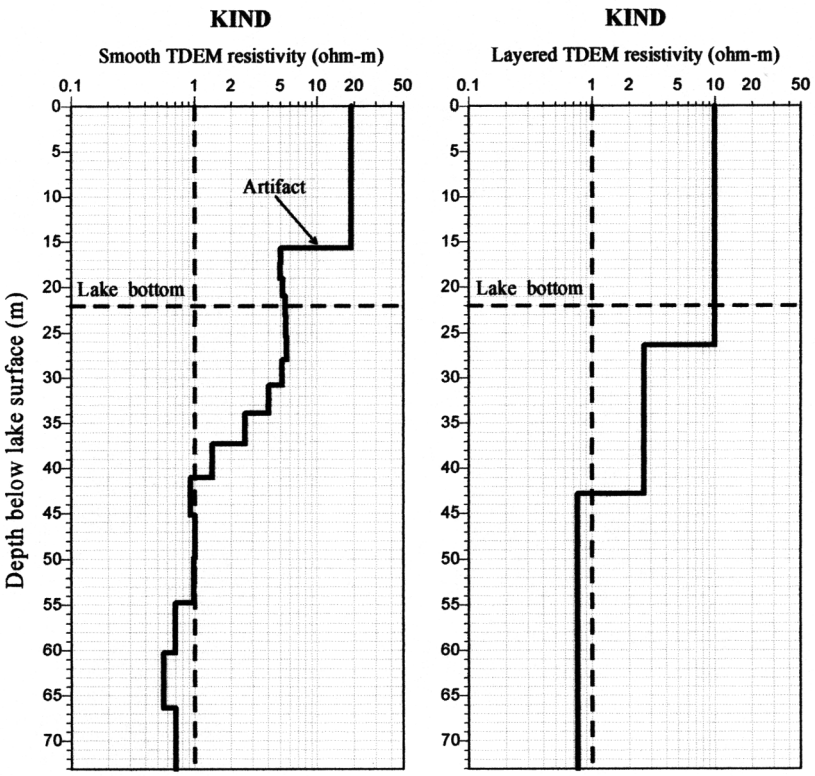

Fig. 6. Layered and smooth models interpreted at station KIND. Vertical dashed line represents threshold resistivity value for brine-saturated sediments. Horizontal dashed line shows the location of the lake bottom.

inversion may have a hydrogeological meaning. Such an approach is in a sense "playing safe", contrary to an alternative "speculative" hydrogeological interpretation of each geoelectric boundary, which could be just an artifact of a non-unique inversion.

TDEM RESULTS

Most of the offshore soundings were acquired along roughly straight lines crossing the lake in both N–S and W–E directions. Some of the profiles have also onshore continuations to distances of up to 1 km from the shore line (Fig. 1). An additional 38 offshore measurements were carried along the coastal line due to a greater variability of the resistivities near the coast. Results are presented both as maps showing the distribution of resistivity at four different depths below the lake's bottom (Fig. 7) and as pseudo-2D resistivity cross sections at selected profiles (Figs. 8 and 9). Both the maps and the cross sections were drawn by interpolation of the interpreted 1-D resistivity models.

The interpreted resistivity values may generally be divided into three major units, each having a distinct spatial distribution.

1. The high resistivity unit has values greater than 4 ohm-m (plotted in dark blue in the maps and cross sections). In the upper part, it obviously includes the water body of the lake (Figs. 8 and 9). The latter, according to the layered inversion, which is more accurate than the smooth inversion for this layer, has values of 7 to 12 ohm-m, usually closer to 10 ohm-m. This figure agrees very well with direct conductivity measurements of the lake water showing conductivity of approximately 100 S/m (A. Katz, personal communication).

   Going deeper, the high resistivity unit covers the entire lake at 5 m depth below the lake bottom (Fig. 7a) and is presented at different parts of the lake in the 10 m map (Fig. 7b). In the 15 m and 20 m maps, the unit appears along most of the lake's perimeter to a distance of approximately 2 km from

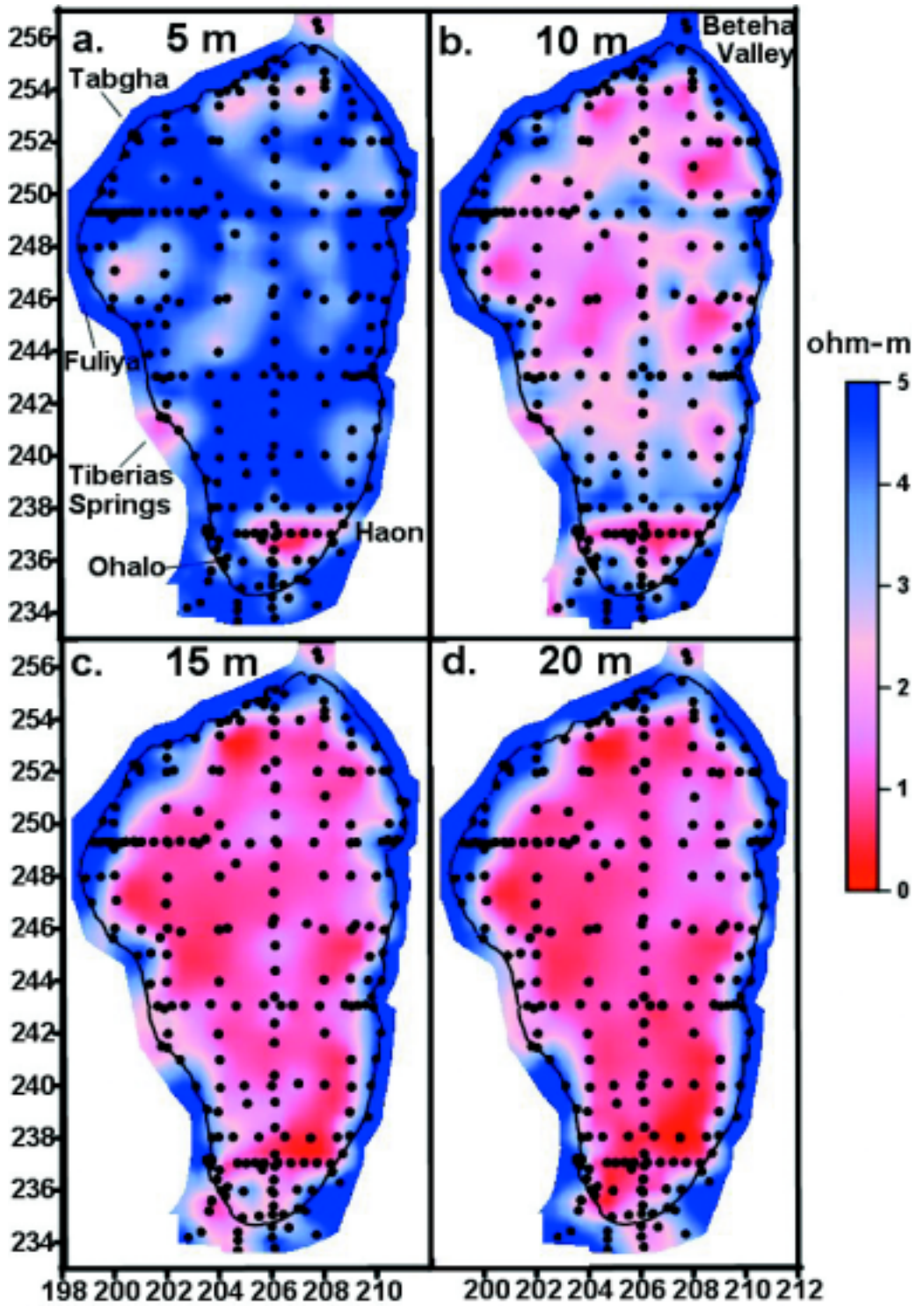

Fig. 7. Distribution of the TDEM resistivities at different depths beneath the bottom of the Lake Kinneret (after Hurwitz et al., 1999). The onshore resistivities are related to depths below the earth surface and are rather schematic, due to the scarcity of the onshore data.

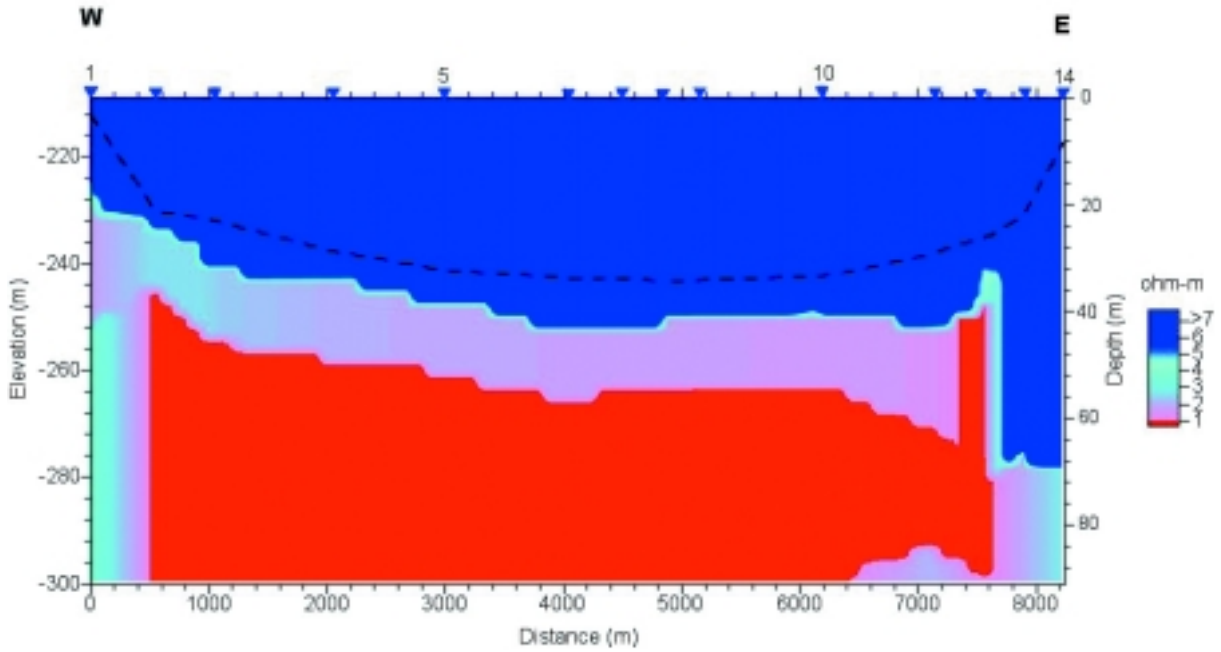

Fig. 8. Quasi-2D resistivity cross section along E5 (Fig. 1) obtained by layered inversion. Dashed line represents lake's bottom.

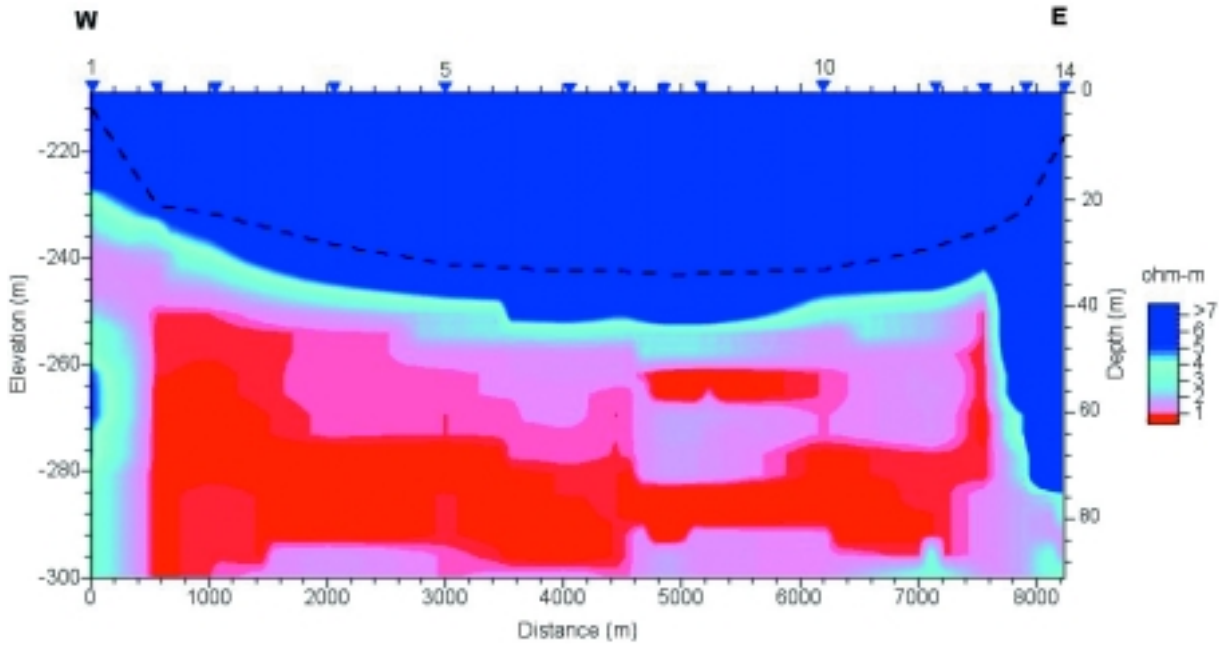

Fig. 9. Quasi-2D resistivity cross section along E5 (Fig. 1) obtained by smooth inversion. Dashed line represents lake's bottom.

the shore, except for areas in the southern and southeastern parts and a small area near Tiberias Springs (Figs. 7c, d).

2. The low resistivity unit represents resistivities below 2 ohm-m. In the 5 m map, it appears in three small areas, adjacent to the Tiberias Springs, Ohalo, and Haon sites (Fig. 7a). In the 10 m map (Fig. 7b), it is exposed at much larger areas, and in the 15 m and 20 m maps, the unit covers most of the internal part of the lake (Figs. 7c, d). The unit appears also onshore as isolated pockets in the Beteha Valley and in the southern shore of the lake.
3. The medium resistivity unit is characterized by resistivities varying between 2 and 4 ohm-m. In most cases it can be identified with the above-mentioned "diffusive transition layer", and it appears throughout the lake at depths of 5 m and 10 m below the bottom and in the margins of the low resistivity unit at greater depths (Figs. 7 a–d).

Figures 8 and 9 show typical examples of quasi-2D resistivity cross sections constructed by interpolation of layered and smooth 1-D models, respectively.

Similar cross sections have been drawn for all six N–S and ten W–E traverses (Fig. 1). Note that the color scales used in the maps and the cross sections are slightly different.

Comparison of Figs. 8 and 9 shows that distribution of resistivities within the smooth cross section is more complicated than that within the layered cross section, although main geoelectric features of the subsurface are similar in both layered and smooth interpretations. Taking into account possible artifacts of smooth inversion, only geoelectric features common for both interpretations are being used in the following hydrogeological discussion. One can see that the most prominent feature of both resistivity cross sections is the geometry of geoelectric layers, which is roughly parallel to the lake bottom in the central part of the traverse and is nearly vertical in both western and eastern margins of the line (Figs. 8 and 9).

RESISTIVITY–SALINITY CALIBRATION

In order to perform hydrogeological analysis of geoelectric results, the interpreted resistivities have to be calibrated by the appropriate borehole salinity measurements. Such resistivity–salinity calibrations have been previously carried out near observation wells at the Mediterranean and Dead Sea coastal aquifers of Israel (Goldman et al., 1991; Kafri et al., 1997). The calibration was carried out by comparison of the borehole salinity data measured at a certain depth with the TDEM resistivity interpreted for the same depth.

Unfortunately, due to the lack of the borehole salinity measurements in the Sea of Galilee, such a procedure is possible at one location only (the Haon-2 well). In order to somehow increase the statistical significance of the calibration, Hurwitz et al. (1999) suggested using the data from long (5 m) cores taken from the lake bottom at three locations throughout the lake (Stiller, 1994; Fig. 3). The salinity data from the cores have been linearly extrapolated to the depths of the low resistivity unit detected by TDEM at the locations of the cores (Fig. 1). The calibration results were surprisingly consistent in all four locations including the Haon-2 well site. Based on these results, the following empirical calibration expression has been suggested: Resistivity (ohm-m) = $4507 \cdot C\ (\text{mg Cl/l})^{-0.9083}$. The expression is valid within the chloride concentration range between 8,000 and 27,000 mg Cl/l.

According to the above expression, a value of 1 ohm-m corresponds to approximately 10,500 mg Cl/l, 1.5 ohm-m corresponds to approximately 6700 mg Cl/l, and 0.5 ohm-m corresponds to a concentration of 22,600 mg Cl/l. Such resistivities are somewhat lower than those obtained in the Mediterranean and Dead Sea coastal aquifers for similar chloridities (Goldman et al., 1991; Kafri et al., 1997). However, the difference is fairly small and falls within the range of the resistivity variations in the coastal aquifers. For example, the resistivity of the seawater-saturated Mediterranean coastal aquifer having chloridity of approximately 18,000 mg Cl/l varies between 0.8 and 2.5 ohm-m with a mean value of 1.6 ohm-m (Goldman et al., 1991). The lower limit of this range roughly coincides with the above calibration data in the Sea of Galilee.

CONCLUSION

The results presented above indicate that the distribution of brines entrapped within the lake's sediments is highly heterogeneous. Most changes, both in brine concentration and depth, are within the 1–2 km zone near the shore. A significant change also occurs between the southern and northern parts of the lake. The maps and cross sections define two zones with different transport mechanisms. Under most parts of the lake, the diffusion is the major transport process (Hurwitz et al., 2000a), whereas, in the margins, the advective flux dominates and diffusion is negligible (Gvirtzman et al., 1997).

In the central part of the lake, the very similar shape of the top low resistivity unit and the lake bottom suggests that in the past, a saline lake covered the area and its water was trapped in the sediments (Hurwitz et al., 2000b). Since the lake was covered with freshwater, diffusion of salts from the sediments into the lake takes place.

In the SE part of the lake, the distance between the top of the low resistivity unit and the lake bottom is small, sometimes negligible. This implies that this part of the lake was covered by the freshwater lake much later than the northern part.

ACKNOWLEDGMENTS

The Israeli Water Commision and the Ministry of National Infrastructures supported the TDEM survey in the Sea of Galilee. We thank Zvi Ben-Avraham who inspired this research. We also thank Michael Ezersky who took part in the data acquisition and preparation of resistivity cross sections. Finally, we want to thank Jacobus Groen for his constructive review.

REFERENCES

Arad, A., Bein, A. 1986. Saline versus freshwater contribution to the thermal waters of the northern Jordan Rift Valley, Israel. Journal of Hydrology 83: 49–66.

Assuline, S., Shaw, M., Rom, M. 1994. The effect of diversion and desalination of the saline springs on the salt concentration in Lake Kinneret and the water addition to the national system. Mekorot Water Company, 44 pp. (in Hebrew).

Ben-Avraham, Z., Ten-Brink, U., Bell, R., Reznikov, M. 1996. Gravity field over the Sea of Galilee: evidence for a composite basin along a transform fault. Journal of Geophysical Research 101: 533–544.

Constable, S.C., Parker, R.L., Constable, C.G. 1987. Occam's inversion: a practical algorithm for generating smooth models from electromagnetic sounding data. Geophysics 52: 289–300.

Fitterman, D.V., Stewart, M.T. 1986. Transient electromagnetic sounding for groundwater. Geophysics 51: 995–1005.

Garfunkel, Z. 1981. Internal structure of the Dead Sea leaky transform (Rift) in relation to plate kinematics. Tectonophysics 80: 81–108.

Goldman, M., Gilad, D., Ronen, A., Melloul, A. 1991. Mapping of seawater intrusion into the coastal aquifer of Israel by the time domain electromagnetic method. Geoexploration 28: 153–174.

Goldman, M., Hurwitz, S., Gvirtzman, H., Rabinovich, B., Rotstein, Y. 1996. Application of the marine time-domain electromagnetic method in lakes: the Sea of Galilee, Israel. European Journal of Environmental and Engineering Geophysics 1: 125–138.

Gvirtzman, H., Garven, G., Gvirtzman, G. 1997. Hydrogeological modeling of the saline hot springs at the Sea of Galilee, Israel. Water Resources Research 33: 913–926.

Hurwitz, S., Goldman, M., Ezersky, M., Gvirtzman, H. 1999. Geophysical (TDEM) delineation of a shallow brine beneath a freshwater lake, the Sea of Galilee, Israel. Water Resources Research 35: 3631–3638.

Hurwitz, S., Lyakhovsky, V., Gvirtzman, H. 2000a. Transient salt transport modeling of a shallow brine beneath a fresh-water lake, the Sea of Galilee. Water Resources Research 36: 101–107.

Hurwitz, S., Stanislavsky, E., Lyakhovsky, V., Gvirtzman, H. 2000b. Transient groundwater-lake interaction in a continental rift: Sea of Galilee, Israel. Geological Society of America Bulletin 112: 1694–1702.

Interpex Limited, 1996. TEMIX-XL user's manual, Vols. 1–2.

Issar, A. 1983. On the source of water from the thermomineral springs of Lake Kinneret (Israel). Journal of Hydrology 60, 175–183.

Kafri, U., Goldman, M., Lang, B. 1997. Detection of subsurface brines, freshwater bodies and the interface configuration in-between by the time domain electromagnetic method (TDEM) in the Dead Sea Rift, Israel. Environmental Geology 31: 42–49.

Marcus, E., Slager, J. 1985. The sedimentary-magmatic sequence of the Zemach 1 well (Jordan–Dead Sea rift, Israel) and its emplacement in time and space. Israel Journal of Earth Sciences 34: 1–10.

Mazor, E., Mero, F. 1969. The origin of the Tiberias-No'it mineral water association in the Tiberias-Dead Sea Rift Valley, Israel. Journal of Hydrology 7: 318–333.

Rimmer, A., Hurwitz, S., Gvirtzman, H. 1999. Spatial and temporal characteristics of saline springs: Sea of Galilee, Israel. Ground Water 37: 663–673.

Shaharabani, M., Michelson, H., Simon, E. 1980. Location of saline flows and seepeges along the eastern shore of Lake Kinneret. TAHAL Report 01/80/30 Tel Aviv, 25 pp. (in Hebrew).

Simon, E., Mero, F. 1992. The salinization mechanism of Lake Kinneret. Journal of Hydrology 138: 327–343.

Stiller, M. 1994. The chloride content in pore water of Lake Kinneret sediments. Israel Journal of Earth Sciences 43: 179–185.